European Journal of Cardio-Thoracic Surgery Advance Access published January 2, 2017

European Journal of Cardio-Thoracic Surgery 00 (2016) 1–7
doi:10.1093/ejcts/ezw393

ORIGINAL ARTICLE

EXPERIMENTAL

Cite this article as: Nauta FJH, de Beaufort HWL, Conti M, Marconi S, Kamman AV, Ferrara A *et al.* Impact of thoracic endovascular aortic repair on radial strain in an *ex vivo* porcine model Eur J Cardiothorac Surg 2016; doi:10.1093/ejcts/ezw393.

Impact of thoracic endovascular aortic repair on radial strain in an *ex vivo* porcine model

Foeke J.H. Nauta[a,b,*], Hector W.L. de Beaufort[a,b], Michele Conti[c], Stefania Marconi[c], Arnoud V. Kamman[a,b], Anna Ferrara[c], Joost A. van Herwaarden[b], Frans L. Moll[b], Ferdinando Auricchio[c] and Santi Trimarchi[a]

[a] Thoracic Aortic Research Center, Policlinico San Donato IRCCS, University of Milan, Italy
[b] Department of Vascular Surgery, University Medical Center Utrecht, the Netherlands
[c] Department of Civil Engineering and Architecture, Beta-lab, University of Pavia, Italy

* Corresponding author. Thoracic Aortic Research Center, Policlinico San Donato IRCCS, University of Milan, Piazza Malan 2, 20097 San Donato Milanese, Milan, Italy. Tel: +39-02-52774344; fax: +39-02-52774383; e-mail: foekenauta@gmail.com (F.J.H. Nauta).

Received 16 June 2016; received in revised form 23 October 2016; accepted 1 November 2016

Abstract

OBJECTIVES: To quantify the impact of thoracic endovascular aortic repair (TEVAR) on radial aortic strain with the aim of elucidating stent-graft-induced stiffening and complications.

METHODS: Twenty fresh thoracic porcine aortas were connected to a mock circulatory loop driven by a centrifugal flow pump. A high-definition camera captured diameters at five different pressure levels (100, 120, 140, 160, and 180 mmHg), before and after TEVAR. Three oversizing groups were created: 0–9% ($n = 7$), 10–19% ($n = 6$), and 20–29% ($n = 6$). Radial strain (or deformation) derived from diameter amplitude divided by baseline diameter at 100 mmHg. Uniaxial tensile testing evaluated Young's moduli of the specimens.

RESULTS: Radial strain was reduced after TEVAR within the stented segment by 49.4 ± 24.0% ($P < 0.001$). As result, a strain mismatch was observed between the stented segment and the proximal non-stented segment (7.0 ± 2.5% vs 11.8 ± 3.9%, $P < 0.001$), whereas the distal non-stented segment was unaffected ($P = 0.99$). Stent-graft oversizing did not significantly affect the amount of strain reduction ($P = 0.30$). Tensile testing showed that the thoracic aortas tended to be more elastic proximally than distally ($P = 0.11$).

CONCLUSIONS: TEVAR stiffened the thoracic aorta by 2-fold. Such segmental stiffening may diminish the Windkessel function considerably and might be associated with TEVAR-related complications, including stent-graft-induced dissection and aneurysmal dilatation. These data may have implications for future stent-graft design, in particular for TEVAR of the highly compliant proximal thoracic aorta.

Keywords: Aortic strain • Stent-graft • Thoracic aorta • TEVAR • Uniaxial tensile testing

INTRODUCTION

Thoracic endovascular aortic repair (TEVAR) is being performed increasingly and its practice is moving towards the arch and the ascending aorta [1, 2]. However, current thoracic stent-grafts are about 125 times stiffer than native thoracic aortic tissue (55.2 vs 0.44 MPa) [3, 4]. Meanwhile, it is known that aortic stiffening predicts cardiovascular mortality [5], as the elasticity of the thoracic aorta serves a critical function in damping the highly pulsatile flow coming from the left ventricle. It allows for flow storage during systole and subsequent release during diastole. This 'Windkessel effect' results in a more continuous flow pattern to the distal vascular beds through the cardiac cycle (Figure 1A) [6]. Preclinical and clinical studies have reported that the replacement of native aortic tissue by a much stiffer endograft fabric can diminish the Windkessel effect, inducing stiffening of both the aorta and the heart, and reducing coronary perfusion [5, 7–12]. The following mechanisms are involved in such adverse cardiovascular remodelling after TEVAR and illustrated in Figure 1:

1. Increased conduit stiffness elevates pulse wave velocity, leading to increased pulse pressure [8, 9, 12] and ventricular afterload, resulting in adverse cardiac remodelling [5, 7].
2. Augmented systolic and reduced diastolic pressures negatively reduce diastolic coronary perfusion [10, 11].

These mechanisms alter the equilibrium between cardiac systolic performance and myocardial diastolic perfusion, leading to an increased risk of long-term heart failure and cardiovascular events [5, 13].

In addition to these systemic effects, local segmental stiffening appears to increase wall stress in adjacent segments, due to a compliance mismatch [14]. Such a mismatch has been reported to weaken the aortic wall, and to be associated with aneurysm formation, retrograde and stent-graft-induced new dissection, or rupture [14–17]. Severe stent-graft oversizing appears to further weaken the

Presented at the American Association for Thoracic Surgery Aortic Symposium, New York, NY, USA, 12-13 May 2016.

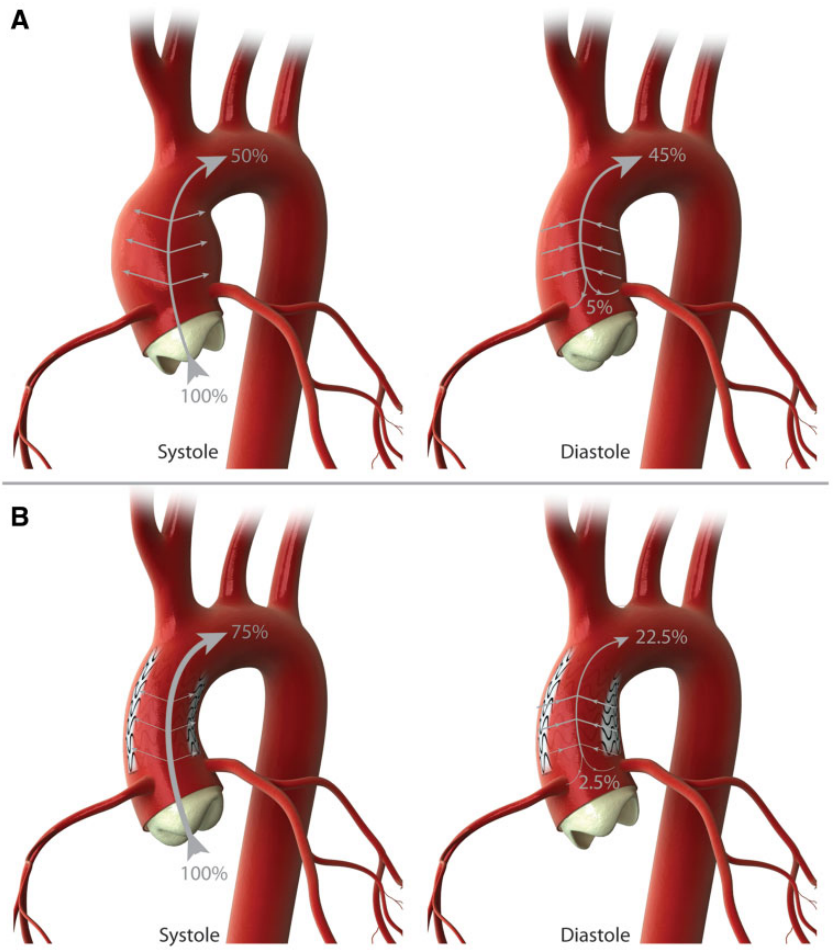

Figure 1: (**A**) The Windkessel effect [6]. During systole the left ventricle ejects 100% of the stroke volume into the thoracic aorta. More or less 50% is directly forwarded towards the distal vascular beds, whereas the other 50% is stored in the expanded aortic lumen. This expansion builds up energy in the elastic aortic wall, which is subsequently used to pump the stored volume to the peripheral circulation and the coronaries. (**B**) The potential effects of ascending TEVAR on the Windkessel effect. In systole, radial strain in the ascending aorta is considerably decreased. Due to this stiffening, the aortic wall's ability to store volume during systole is diminished and most of the stroke volume is directly forwarded. During diastole, less flow is available for diastolic perfusion of the peripheral vasculature, including the coronaries [10, 11]. Moreover, the stiffened aorta elevates pulse pressures [5, 8, 9, 12], leading to increased ventricular afterload with subsequent cardiac remodelling [5, 7].

aortic wall proportional to the degree of oversizing, due to subacute changes in biomechanical aortic properties [18]. This was shown in porcine aortas after removal of the stent-graft. However, the effect of stent-graft oversizing on radial strain in a stented aorta is unclear and may provide insights in aortic stiffening in relation to oversizing.

Recently, our group reported decreased longitudinal strain following TEVAR in an experimental setup using porcine aortic tissue and a mock circulatory loop [19]. To date, the impact of TEVAR on radial strain remains undetermined. Motivated by the lack of data and the potential important clinical consequences, we aimed to quantify radial strain before and after TEVAR using the same *ex vivo* isolated porcine model, with particular attention to stent-graft oversizing. In addition, we assessed elastic properties through uniaxial tensile testing to assess homogeneity of the used specimens and to identify potential vulnerable aortic segments.

MATERIALS AND METHODS

Aortic specimens

Twenty fresh porcine thoracic aortas (healthy Goland pigs, commercial hybrid, of 10–12 months old and 160–180 kg) were collected from a local slaughterhouse. No pigs were sacrificed solely for this study and ethical permission was not required by the local ethical committee. The aortas were transported on iced 0.9% saline solution (transport time of 30 min) and all measurements were conducted within 12 h from death to ensure the use of fresh specimens. As the ascending aorta of pigs measures only 2–3 cm, we used the distal arch (with a length of 3 cm) and descending aorta (with a length of 32.5 cm) for these experiments. Specimens were procured from the left subclavian artery till the celiac trunk and all side branches were ligated. Prior to the experiments, the aortas were bathed in 0.9% saline of room temperature (about 20°C) for 15 min. The complete study protocol has been published before [19].

Mock circulatory loop

The aortas were connected to a mock circulatory loop driven by a centrifugal flow pump (Medtronic Bioconsole BIO-MEDICUS 550, Minneapolis, MN, USA). This allowed for controlled intraluminal pressurization. To preserve the biomechanical characteristics of the nitinol stents [20], water at body temperature was used (using a liquid heater; Nova Powerstat Protonic®, Boise, ID, USA).

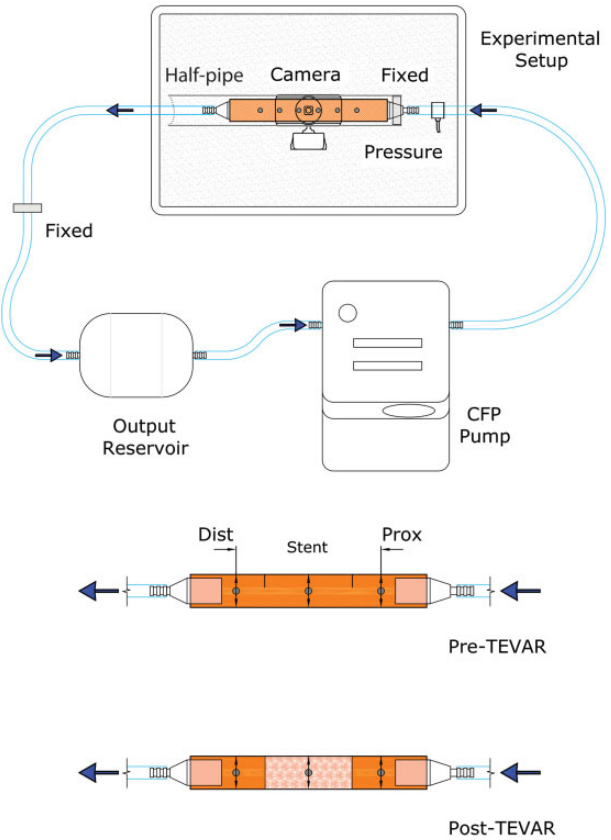

Figure 2: Schematic of the mock circulatory loop system. Top: The CFP propels the water through a soft silicon tube into the porcine aorta. 'Fixed' marks the locations where the tube is fixed and 'Pressure' shows the location of the pressure sensor. 'Camera' illustrates the location of the HD-camera. The 'Output Reservoir' is the water reservoir that supplies the CFP. Bottom: 'Pre-TEVAR' shows the situation before TEVAR with the proximal, stented, and distal levels marked accordingly. 'Post-TEVAR' illustrates the situation after TEVAR, including the implanted stent-graft. CFP: centrifugal flow pump; Dist: distal; Prox: proximal; Stent: stented.

Intraluminal pressures were constantly recorded using a pressure sensor (Micro Switch Pressure Sensor 40PC Series Chart, Honeywell, Freeport, IL, USA) that was connected to a fixed silicon tube, just proximal to the aorta. Distally, the aorta was connected to a silicon tube that could move against low, standardized, resistance through a guiding half-pipe (Figure 2). A prestress of 100 mmHg (mean blood pressure in pigs) [21] was applied for all aortas prior to diameter measurements.

Radial strain calculations

The aortas were marked with a superficially sutured rubber dot to identify intersections of interest; 5 cm proximal to the stent-graft, in the middle of the stented segment, and 5 cm distal to the device. Using a high-definition webcam (Logitech HD Pro Webcam C920, Lausanne, Switzerland), snapshots (1920 × 1080 pixels) were conducted at five different pressure moments; 100, 120, 140, 160, and 180 mmHg. All photos were post-processed using a custom developed computer script made with Matlab (The MathWorks©, Inc., Natick, MA, USA). The script showed the investigator each image of the dataset to manually measure aortic diameters at the marked sections, perpendicular to the aortic wall. Mean diameter and radius were computed for each level independently by two investigators (F.N. and H.B., research fellows in aortic disease) to allow for intra- and interobserver agreement analysis. Radial aortic strain was calculated as:

$$\text{Radial strain} = \frac{\text{Radius at appointed pressure} - \text{Radius at 100mmHg}}{\text{Radius at 100mmHg}} * 100\%$$

Stent-graft implantation

Medtronic Valiant stent-grafts (Medtronic Vascular, Santa Rosa, CA, USA) with a length of 150 mm were implanted with a custom-developed loading and deployment system. To study the impact of stent-graft oversizing, three groups of oversizing were created; 0–9% ($n = 7$), 10–19% ($n = 7$), and 20–29% ($n = 6$). Stent-graft sizing was based on adventitia–adventitia diameters at the proximal landing zone, 5 cm distal to the left subclavian artery. These diameters were measured twice by two investigators (F.N. and M.C., engineer in aortic device development) with an electronic calliper, of which mean values were used for analysis.

Uniaxial tensile testing

Directly following the radial strain measurements, all specimens were preserved in a refrigerator at ∼7°C. Subsequently, maximum elastic moduli of the aortic specimens were assessed through uniaxial tensile testing [22] by Day 2 after pig sacrifice (1.5 ± 0.8 days), minimizing the impact of delay and storage on the mechanical response of the tissue. The aortas were incised along the posterior wall to explant the stent-graft. The preserved anterior aortic wall was then used for tensile testing as this was free of spinal side branches. Three zones of interest were distinguished in the excised thoracic aorta, i.e. proximal, stented, and distal. A bone-shaped specimen cutter extracted circumferential bone-shaped strips from the aortic tissue. These specimens were used for the tensile tests, which was performed by an MTS Insight Testing System 10 kN (MTS System Corporation, Eden Prairie, MN, USA) equipped with a 250 N load-cell, and by a ME-46 Video Extensometer (Messphysik, Fürstenfeld, Austria). Elastic moduli derived from stress–strain curves and peak stress-to-rupture were quantified as peak stress needed to rupture the specimen.

Statistical analysis

Data are shown as frequencies, percentages, and mean ± standard deviation, where appropriate. Grubb's testing identified outliers ($\alpha = 0.05$), which were excluded from the analysis. Shapiro–Wilk testing was used to test the normality of data distribution. Statistical significance was evaluated with two-tailed paired *t*-tests or one-way analysis of variance. Intra- and interobserver agreement of aortic diameters was assessed through Lin's concordance correlation coefficient method (LCCC). An LCCC of <0.90 was deemed as poor, 0.90–0.95 as moderate, 0.95–0.99 as substantial, and >0.99 as almost perfect agreement.

RESULTS

Time between pre-TEVAR and post-TEVAR measurements was 0.6 ± 0.2 h. Time of delay between harvesting of the aorta and the

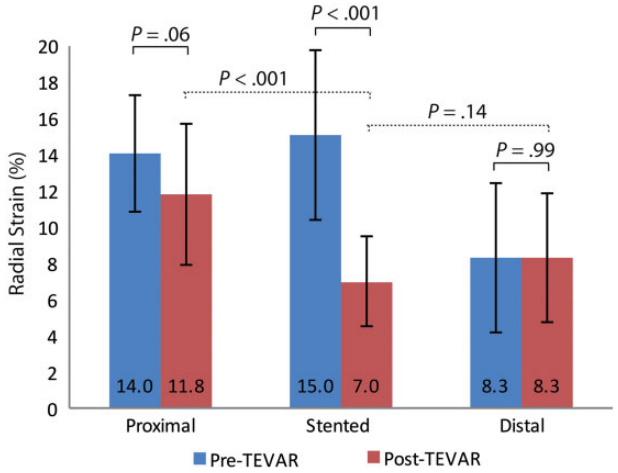

Figure 3: Maximum radial strain between 100–180 mmHg pre- and post-TEVAR in the proximal, stented, and distal segments ($n = 20$).

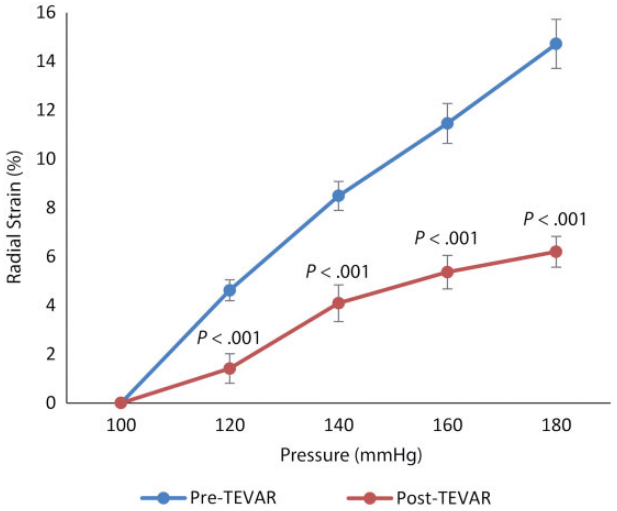

Figure 4: Radial strain in the stented segments pre- and post-TEVAR along rising pressure ($n = 20$).

initiation of the experiment was 7.1 ± 2.6 h and the water temperature was 37.2 ± 0.2°C. Mean diameter at the proximal landing zone was 20.5 ± 0.9 mm, pressurized at 100 mmHg.

Radial strain changes after thoracic endovascular aortic repair

Mean radial strains ($n = 20$) before and after TEVAR are shown in Figure 3. In the stented segments, radial strain decreased from a mean 15.0 ± 4.7% before TEVAR to a mean 7.0 ± 2.5% after TEVAR, a 2-fold reduction, on average 49%, which was statistically significant ($P < 0.001$). The proximal segment also tended to show a decrease of radial strain ($P = 0.06$), whereas radial strain in the distal segment remained unchanged ($P = 0.99$).

Figure 4 demonstrates radial strain along increasing pressure in the stented segments, before and after TEVAR. The reduction in radial strain after TEVAR was significant for each pressure condition ($P < 0.001$ for 120, 140, 160, and 180 mmHg) and the size of the reduction caused by TEVAR increased as pressure rose ($P < 0.001$).

Impact of stent-graft oversizing on radial strain

Figure 5 illustrates radial strain before and after TEVAR per oversizing group. There were no baseline differences in radial strain between oversizing groups ($P = 0.64$). After TEVAR, radial strain in the stented segments decreased in all oversizing groups ($P < 0.001$ for all groups). Stent-graft oversizing did not affect the amount of strain reduction, which was 60.9 ± 21.6% in the 0–9% oversizing group, 46.0 ± 27.7% for the 10–19% oversizing group, and 40.2 ± 22.7% when the device was oversized with 20–29% ($P = 0.30$). Regarding strain after TEVAR in the proximal and distal adjacent segments, no significant differences in strain reduction were found among the oversizing groups ($P = 0.87$ and $P = 0.40$, respectively).

Radial strain mismatch following thoracic endovascular aortic repair

After TEVAR, a significant radial strain mismatch was observed between the stented and proximal non-stented thoracic aortas

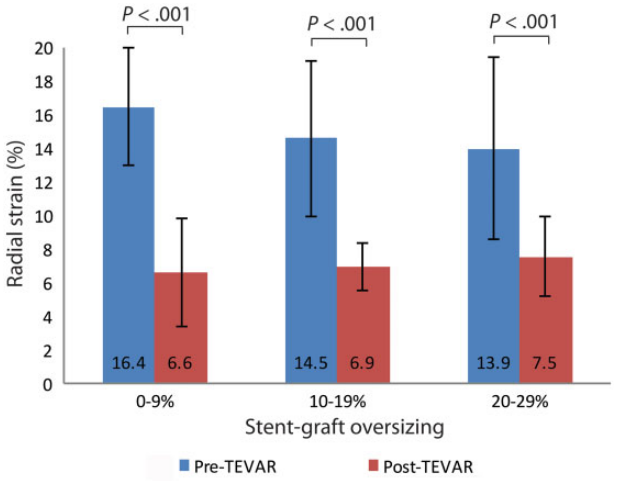

Figure 5: Maximum radial strain between 100–180 mmHg in the stented segments for the oversizing groups 0–9% ($n = 7$), 10–19% ($n = 6$), and 20–29% ($n = 6$), pre- and post-TEVAR.

(Figure 3, $P < 0.001$). The distal adjacent segment showed no statistically significant radial strain mismatch, although a trend was observed ($P = 0.14$).

Uniaxial tensile testing

Uniaxial tensile testing demonstrated that the aortic specimens used in this study were homogenous regarding circumferential maximum Young's moduli (26.1 ± 10.3 MPa, coefficient of variation = 41.4%). Figure 6A shows maximum Young's moduli in the proximal, stented (central), and distal segments. Elasticity was similar along the different segments ($P = 0.41$), although the proximal end tended to be more elastic than the distal segment ($P = 0.11$). The elasticity of the stented segment was comparable to the distal segment ($P = 0.22$).

Following stent-graft explant, we observed stent markers in the intima along the stented segment (Figure 6B), without macroscopic differences among oversizing groups. Moreover, tensile testing showed no significant differences of maximum Young's

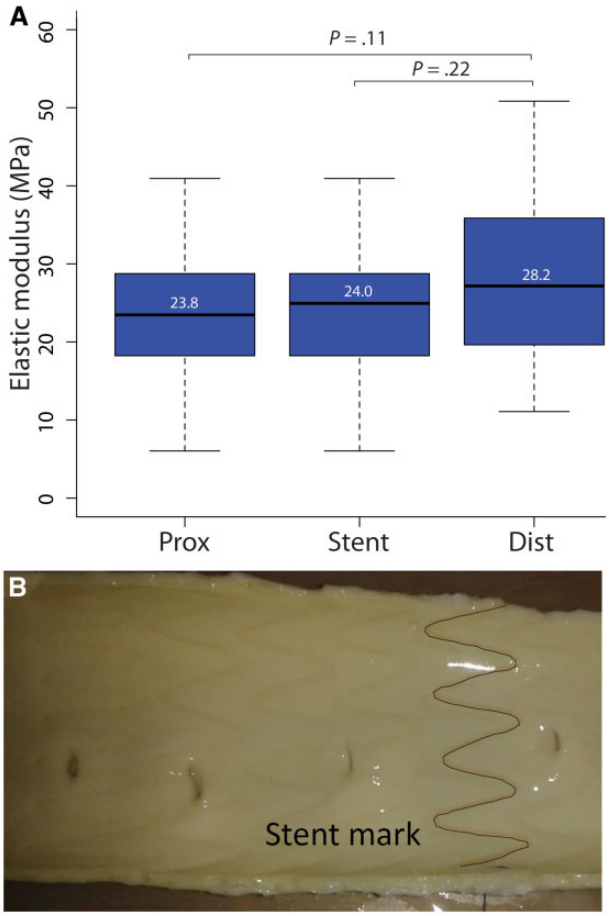

Figure 6: Uniaxial tensile testing ($n = 20$). (**A**) Mean maximum elastic moduli per zone. (**B**) Stent marks along the intima of the thoracic porcine aorta. Dist, distal; Prox, proximal; Stent, stented.

moduli ($P = 0.23$) and stress-to-rupture rates ($P = 0.89$) in the stented segment when comparing the three oversizing groups.

Intra- and interobserver agreement

For intraobserver measurements, mean diameter differences ± SD were 0.10 ± 0.55 mm before TEVAR and 0.07 ± 0.60 mm after TEVAR, with LCCCs of 0.96 (95% CI, 0.89–0.99) and 0.96 (95% CI, 0.90–0.98), respectively. This indicated substantial intraobserver agreement. Regarding interobserver measurements, mean diameter differences ± SD were 0.30 ± 0.83 mm before TEVAR and 0.27 ± 0.49 mm with LCCCs of 0.92 (95% CI, 0.80–0.97) and 0.96 (95% CI, 0.90–0.98), respectively. This indicated moderate-to-substantial interobserver agreement.

DISCUSSION

Segmental stiffening by a stent-graft seems to predominantly shift the adverse effects up-stream to the heart in a retrograde fashion. Increased impedance in the descending aorta increases left ventricular workload with ventricular stiffening as result [7, 8], which is an established predictor of cardiovascular events and death [5]. In addition to such systemic adverse effects, there may be a local compliance mismatch between a stiff stent-graft and a more elastic aorta, as reported in this study. This mismatch has been suggested to play a role in important complications such as retrograde aortic dissection, aneurysmal dilatation, rupture, and stent-graft-induced new entry tears. However, the rate of aortic stiffening following TEVAR remains unclear. To elucidate this, we studied the impact of TEVAR on radial aortic strain in an experimental model using porcine aortas and a mock circulatory loop. Our main finding was that TEVAR reduced radial aortic strain by 2-fold. This suggests that TEVAR diminishes the Windkessel effect considerably, because radial deformation is the main determinant of volume expansion [6]. Moreover, we found that TEVAR-induced radial stiffening resulted in a radial strain mismatch in the proximal thoracic aorta. This has been associated with elevated wall stress and weakening of the aortic wall, increasing the risk of aneurysmal dilatation and aortic dissection [14–17].

We observed radial strain rates of about 14–15% in the proximal descending porcine aorta, corresponding to strains in the healthy ascending adult aorta [23]. Our results may therefore predominantly apply to the human ascending aorta. It is well reported that replacement of the ascending aorta with a surgical Dacron graft decreases compliance by about 30%, leading to increased impedance and left ventricle hypertrophy [24, 25]. However, these effects remain unclear for TEVAR. Our finding that TEVAR appears to reduce the Windkessel function by about 50% is timely and important as indications for endovascular repair are currently expanding to address proximal aortic pathology [2]. Figure 1B illustrates the potential effects of stent-graft-induced modification of the Windkessel effect. Following TEVAR, the aortic wall's ability to store volume during systole is diminished and most of the stroke volume is directly forwarded. As result, less flow is available for diastolic perfusion of the peripheral vasculature, including the coronaries. Moreover, due to conduit stiffening just distal to the aortic valve, a significant increase of pulse pressure is expected [5, 8, 9], leading to elevated cardiac afterload and cardiac remodelling [5, 7], and reduced coronary perfusion [10, 11]. However, these potential effects of TEVAR should be confirmed in *in vivo* studies.

In this experimental study, stent-graft oversizing did not significantly affect the reduction of radial strain after TEVAR. We observed that the highest oversizing group (20–29%) tended to show the lowest reduction of radial strain in the stented segments. This finding might be explained by the severe oversizing that creates a certain level of stent-graft infolding, resulting in higher radial strains at rising pressures due to unfolding. Yet, this remains speculative. Importantly, severe stent-graft oversizing is not recommended due to weakening of the wall and increased risks of complications [18].

We observed a significant proximal radial strain mismatch following TEVAR. It has been reported that such a local mismatch increases wall stress [14]. With each cardiac cycle, the aortic wall experiences this elevated stress, which eventually weakens the artery. The results of our experimental setup might even underestimate the impact of TEVAR on radial strain as the *in vivo* adjacent aortic segments most likely will compensate for the increased impedance in the stented segments, further increasing the mismatch [14]. Importantly, although young patients are not likely candidates for stent-grafting, trauma patients that suffer from an aortic lesion are often young of age with otherwise normal hearts and aortas. Such patients are increasingly managed with stent-grafts and the stiffening effects induced by TEVAR are markedly profound in this cohort, as their hearts and aortas are more compliant [4, 9].

With rising pressure, radial strain was significantly reduced. This suggests that potential adverse stiffening effects of stent-grafts

worsen in case of hypertension, which emphasizes the importance of strict blood pressure regulation following TEVAR. This supports suggestions by others stating that perioperative hypertension may increase the risk of aortic dissection [26].

Tensile testing showed that the thoracic aortas tended to be more elastic proximally than distally, in agreement with literature [27]. This finding further underlines the high elasticity of the proximal thoracic aorta. This observation is relevant in the current era of proximal TEVAR and might have implications for future stent-graft designs.

Study limitations

The following limitations are important to be addressed when interpreting the results. At first, we acknowledge that the use of porcine aortic tissue is a limitation. However, porcine tissue is commonly used in cardiovascular research [28] as their mechanical properties are comparable to young human tissue [29] and because they are more widely available than human cadaveric samples. Nonetheless, healthy porcine aortic tissue is more elastic than aged human aortic tissue [4, 19]. Additional *in vivo* studies in aged humans are therefore warranted to translate these experimental findings to clinical practice. Secondary, we used a simplified static pressure circulatory model. Although this model neglected dynamic effects that may occur owing to cyclic systolic–diastolic wall deformations, such an experimental, controlled setup has repeatedly been used to assess new biomechanical concepts and assess aortic mechanical properties [14]. Moreover, we found comparable radial strain rates when compared with pulsatile *ex vivo* experimental and *in vivo* patient studies [23, 28]. A third limitation of this study is the use of non-thrombotic blood analogue. This was chosen because a thrombotic agent rapidly led to clotting in the mechanical pump, because there are no epithelial cells to inhibit this. Besides, such non-thrombotic fluids do not have relevant influence on the high-speed condition of the aorta [30]. Therefore, we used water to pressurize the aortas, similarly to other *ex vivo* haemodynamic studies [28]. We also note that our findings only apply for Medtronic Valiant stent-grafts, which have interrupted stents. Other stent-graft designs might show different radial strain rates.

CONCLUSION

TEVAR stiffened the thoracic aorta in the radial direction by 2-fold, creating a significant strain mismatch between the stented and proximal non-stented thoracic aortas. Such TEVAR-induced aortic stiffening may very well diminish the Windkessel function, increasing pulse pressure and cardiac afterload, with risk of hypertension, adverse cardiac remodelling, and reduced coronary perfusion. Moreover, such a local radial strain mismatch is associated with elevate wall stress and increased risk of aortic complications including aneurysmal dilatation and post-TEVAR aortic dissection. This study contributes to the understanding on the impact of TEVAR on proximal thoracic aortic dynamics, with potential implications for future stent-graft design.

Funding

This work was supported by ERC Starting Grant through the Project ISOBIO: Isogeometric Methods for Biomechanics [259229]; iCardioCloud project by Cariplo Foundation [2013-1779]; and Lombardy Region [42938382, 46554874].

Conflict of interest: none declared.

REFERENCES

[1] von Allmen RS, Anjum A, Powell JT. Incidence of descending aortic pathology and evaluation of the impact of thoracic endovascular aortic repair: a population-based study in England and Wales from 1999 to 2010. Eur J Vasc Endovasc Surg 2013;45:154–9.
[2] Piffaretti G, Galli M, Lomazzi C, Franchin M, Castelli P, Mariscalco G, *et al.* Endograft repair for pseudoaneurysms and penetrating ulcers of the ascending aorta. J Thorac Cardiovasc Surg 2016;151:1606–14.
[3] Kleinstreuer C, Li Z, Basciano CA, Seelecke S, Farber MA. Computational mechanics of Nitinol stent grafts. J Biomech 2008;41:2370–8.
[4] Roccabianca S, Figueroa CA, Tellides G, Humphrey JD. Quantification of regional differences in aortic stiffness in the aging human. J Mech Behav Biomed Mater 2014;29:618–34.
[5] Benetos A, Safar M, Rudnichi A, Smulyan H, Richard JL, Ducimetieère P *et al.* Pulse pressure: a predictor of long-term cardiovascular mortality in a French male population. Hypertension 1997;30:1410–5.
[6] Belz GG. Elastic properties and {Windkessel} function of the human aorta. Cardiovasc Drugs Ther 1995;9:73–83.
[7] Takeda Y, Sakata Y, Ohtani T, Tamaki S, Omori Y, Tsukamoto Y *et al.* Endovascular aortic repair increases vascular stiffness and alters cardiac structure and function. Circ J 2014;78:322–8.
[8] Dobson G, Flewitt J, Tyberg JV, Moore R, Karamanoglu M. Endografting of the descending thoracic aorta increases ascending aortic input impedance and attenuates pressure transmission in dogs. Eur J Vasc Endovasc Surg 2006;32:129–35.
[9] Tzilalis VD, Kamvysis D, Panagou P, Kaskarelis I, Lazarides MK, Perdikides T *et al.* Increased pulse wave velocity and arterial hypertension in young patients with thoracic aortic endografts. Ann Vasc Surg 2012;26:462–7.
[10] Zacharoulis AA, Arapi SM, Lazaros GA, Karavidas AI, Zacharoulis AA. Changes in coronary flow reserve following stent implantation in the swine descending thoracic aorta. J Endovasc Ther 2007;14:544–50.
[11] Watanabe H, Ohtsuka S, Kakihana M, Sugishita Y. Coronary circulation in dogs with an experimental decrease in aortic compliance. J Am Coll Cardiol 1993;21:1497–506.
[12] Lantelme P, Dzudie A, Milon H, Bricca G, Legedz L, Chevalier J-M *et al.* Effect of abdominal aortic grafts on aortic stiffness and central hemodynamics. J Hypertens 2009;27:1268–76.
[13] Bluemke DA, Kronmal RA, Lima JAC, Liu K, Olson J, Burke GL *et al.* The relationship of left ventricular mass and geometry to incident cardiovascular events: the MESA (Multi-Ethnic Study of Atherosclerosis) study. J Am Coll Cardiol 2008;52:2148–55.
[14] Raaz U, Zöllner AM, Schellinger IN, Toh R, Nakagami F, Brandt M *et al.* Segmental aortic stiffening contributes to experimental abdominal aortic aneurysm development. Circulation 2015;131:1783–95.
[15] Dong ZH, Fu WG, Wang YQ, Guo DQ, Xu X, Ji Y, *et al.* Retrograde type A aortic dissection after endovascular stent graft placement for treatment of type B dissection. Circulation 2009;119:735–41.
[16] Dong Z, Fu W, Wang Y, Wang C, Yan Z, Guo D, *et al.* Stent graft-induced new entry after endovascular repair for Stanford type B aortic dissection. J Vasc Surg 2010;52:1450–7.
[17] Humphrey JD, Holzapfel GA. Mechanics, mechanobiology, and modeling of human abdominal aorta and aneurysms. J Biomech 2012;45:805–14.
[18] Sincos IR, Aun R, da Silva ES, Belczak S, de Lourdes Higuchi M, Gornati VC *et al.* Impact of stent-graft oversizing on the thoracic aorta: experimental study in a porcine model. J Endovasc Ther 2011;18:576–84.
[19] Nauta FJH, Conti M, Marconi S, Kamman AV, Alaimo G, Morganti S *et al.* An experimental investigation of the impact of thoracic endovascular aortic repair on longitudinal strain. Eur J Cardiothorac Surg 2016;50:955–61.
[20] Robich MP, Hagberg R, Schermerhorn ML, Pomposelli FB, Nilson MC, Gendron ML *et al.* Hypothermia severely effects performance of nitinol-based endovascular grafts in vitro. Ann Thorac Surg 2012;93:1223–7.
[21] Hannon JP, Bossone CA, Wade CE. Normal physiological values for conscious pigs used in biomedical research. Lab Anim Sci 1990;40:293–8.
[22] Ferrara A, Morganti S, Totaro P, Mazzola AAF. Human dilated ascending aorta: mechanical characterization via uniaxial tensile tests. J Mech Behav Biomed Mater 2016;53:257–71.

[23] Bell V, Mitchell WA, Sigurðsson S, Westenberg JJM, Gotal JD, Torjesen AA *et al.* Longitudinal and circumferential strain of the proximal aorta. J Am Heart Assoc 2014;3:e001536.
[24] Morita S, Asou T, Kuboyama I, Harasawa Y, Sunagawa K, Yasui H. Inelastic vascular prosthesis for proximal aorta increases pulsatile arterial load and causes left ventricular hypertrophy in dogs. J Thorac Cardiovasc Surg 2002;124:768–74.
[25] Kim SY, Hinkamp TJ, Jacobs WR, Lichtenberg RC, Posniak H, Pifarré R. Effect of an inelastic aortic synthetic vascular graft on exercise hemodynamics. Ann Thorac Surg 1995;59:981–9.
[26] Fattori R, Lovato L, Buttazzi K, Di Bartolomeo R, Gavelli G. Extension of dissection in stent-graft treatment of type B aortic dissection: lessons learned from endovascular experience. J Endovasc Ther 2005;12:306–11.
[27] Khanafer K, Duprey A, Zainal M, Schlicht M, Williams D, Berguer R. Determination of the elastic modulus of ascending thoracic aortic aneurysm at different ranges of pressure using uniaxial tensile testing. J Thorac Cardiovasc Surg 2011;142:682–6.
[28] Krüger T, Grigoraviciute A, Veseli K, Schibilsky D, Wendel HP, Schneider W, *et al.* Elastic properties of the young aorta: ex vivo perfusion experiments in a porcine model. Eur J Cardiothorac Surg 2015;48:221–7.
[29] Li W-C, Yu M-H, Zhang H-M, Wang H-Q, Xi G-M, Yao B-C, *et al.* Biomechanical properties of ascending aorta and pulmonary trunk in pigs and humans. Xenotransplantation15:384–9.
[30] Liu X, Fan Y, Deng X, Zhan F. Effect of non-Newtonian and pulsatile blood flow on mass transport in the human aorta. J Biomech 2011;44:1123–31.